INTERFERENCE STATISTICS IN A RANDOM MMWAVE AD HOC NETWORK

Andrew Thornburg, Tianyang Bai, and Robert W. Heath, Jr.

Wireless Communication and Networking Group
The University of Texas at Austin
1616 Guadalupe St, UTA 7.518, Austin, TX 78701

ABSTRACT

Wireless communication at millimeter wave (mmWave) frequencies is attractive for cellular, local area, and ad hoc networks due to the potential for channels with large bandwidths. As a byproduct of directional beamforming and propagation differences, some studies have claimed that mmWave networks will be noise rather than interference limited. This paper presents a derivation of the instantaneous interference-to-noise ratio (INR) distribution of a mmWave ad hoc network. Random network model of transmitters represented by a Poisson point process with a narrowband channel model is used to derive an approximation of the INR distribution. The analysis shows that the shape of the INR distribution is determined largely by the line-of-sight interferers, which depends on the overall network density and building blockage. A main conclusion drawn is that even with highly directional beamforming, interference can only sometimes be neglected in an ad hoc network. With a reasonable choice of system parameters, the interference is nearly always stronger than the noise power in dense networks.

1. INTRODUCTION

The millimeter wave (mmWave) spectral band is used for personal and local area networks [1, 2], and is under consideration for cellular networks [3, 4]. The potential for high bandwidth channel allocations also makes mmWave technology attractive for ad hoc networking. Such communication is already supported in personal area network standards in small indoor areas [1, 2, 5]. Two distinguishing features of communication at mmWave relative to lower frequencies are the use of beamforming with large antenna arrays and extreme sensitivity to blockages in the environment. These features change the statistics of the interference experienced at mmWave receivers.

Different claims are made in prior work about the sensitivity of mmWave networks to interference. Some work on personal area networks argues that they will be largely noise limited [6], while other work argues that smart scheduling is needed to manage interference [7]. Similar conclusions are drawn in work on cellular communication where some claim that mmWave is noise limited [4] while others claim that it is interference limited [3]. The analysis in [3] shows that mmWave cellular networks operate in the spectrum between interference limited and noise limited as a function of the density of the environment. Unfortunately, there is no such analysis using a comparable analytical framework for outdoor ad hoc networks in the presence of large scale blockage. Therefore it is not clear whether ad hoc networks are more likely to operate in interference limited or noise limited regimes.

In this paper, we derive a tight approximation on the instantaneous interference to noise ratio (INR) for outdoor mmWave ad hoc networks. We consider a narrowband channel model with transmitter locations forming a Poisson point process. We incorporate mmWave features by using directional beamforming and acccounting for the difference between LOS and NLOS interference. Because of the sensitivity of mmWave RF propagation to blockage from buildings and humans [8], line-of-sight (LOS) links tend to have a much lower path-loss exponent than non-line-of-sight (NLOS) links. We show that in *dense* networks the interference power is nearly always higher than the noise power. For sparse networks with narrow antenna patterns, the network is indeed noise limited. We further show that the INR distribution is heavily determined by the LOS interference which is why we call mmWave ad hoc network *LOS interference limited*. This motivates further work for practical mmWave transmitter/receiver structures to reduce the, often powerful, LOS interference.

2. SYSTEM MODEL

Consider an ad hoc network where each transmitter is a point of a Poisson point process (PPP) with density λ. We consider a narrowband signal model. This is justified through the potential use of ODFM, as is considered in the mmWave 802.11ad standard [1]. We analyze interference at the *typical* receiver located at the origin. We use the *dipole* model which assumes each transmitter has an associated receiver at distance R [9]. By Slivynak's Theorem [9], conditioning on a typical receiver at the origin, all the other transmitters still form a PPP. The typical receiver observes the SINR defined

The authors would like to acknowledge support from Army Research Labs under Grant No. W911NF-12-R-0011 and the National Science Foundation under Grant No. 1218338

as

$$\text{SINR} = \frac{P_{\text{t}} M_0 h_0 A R^{-\alpha_0}}{N_0 + \sum_{\text{i}\in\Phi} P_{\text{t}} M_{\text{i}} h_{\text{i}} A r_{\text{i}}^{-\alpha_{\text{i}}}} \tag{1}$$

where P_{t} is the transmit power (no power control is considered), M_0 is the antenna gain corresponding to gain between the typical receiver and transmitter, h_0 is the fading power at the typical receiver, R is the fixed link length between a transmitter and its associated receiver, A is the path-loss intercept, α_0 is the path-loss exponent for the desired signal, α_{i} is the path-loss exponent between each transmitter and the receiver, and N_0 is the noise power. The terms within the sum are for each interfering transmitter; r_i is used to represent the distance from the interferer to the typical receiver, h_{i} is each interferer fading power, and M_{i} is the discrete random antenna gain, explained below [10]. For the analysis in this paper, we focus on the interference to noise ratio defined as

$$\text{INR} = \frac{\sum_{\text{i}\in\Phi} P_{\text{t}} M_{\text{i}} h_{\text{i}} A r_{\text{i}}^{-\alpha_{\text{i}}}}{N_0}. \tag{2}$$

Next, we elaborate on the rationale of the antenna gain, path-loss exponent, and fading power.

To achieve a sufficient link margin, mmWave devices use directional antennas [11]. We approximate the actual beam pattern of the antennas as a sectored model, as used in [12] and shown in Fig. 1. The beam pattern is parameterized by three values: main lobe beamwidth (θ), main lobe gain (M), and back lobe gain (m) [3, 10]. Each interfering transmitter uses its direction antenna to direct the RF energy towards the intended receiver. Because in the sectored antenna model each antenna pattern has 2 discrete possibilities, the resulting antenna gain at the *typical* receiver is a uniform variable described over $[0, 2\pi]$. We model this as a discrete random variable described by

$$M_{\text{i}} = \begin{cases} MM & \text{w.p. } \; p_{\text{MM}} = (\frac{\theta}{\pi})^2 \\ Mm & \text{w.p. } \; p_{\text{Mm}} = 2\frac{\theta}{\pi}\frac{\pi-\theta}{\pi} \\ mm & \text{w.p. } \; p_{\text{mm}} = (\frac{\pi-\theta}{\pi})^2 \end{cases}. \tag{3}$$

Furthermore, we assume that the typical dipole performs perfect beam alignment and thus has an antenna gain of MM. We note that the sectored model is pessimistic with regards to side band power. A typical uniform linear array, for instance, will consist of a main-lobe and many less powerful side-lobes each separated by nulls. The sectored model takes the most powerful side-lobe as the entire side-lobe (i.e. on average, the sectored model provides higher side-lobe power). We believe incorporating side-lobe power is an important distinction as well. Other work ignores the side-lobe power [6]. While outdoor, mobile mmWave devices will use directional antennas, due to practical issues like movement and beam-tracking, we do not expect extremely small, *pencil* beams. We analyze the interference power over three beamwidths: 9°, 30°, and 90°.

We consider an outdoor, urban type environment. As such, the interference experienced at the *typical* receiver at

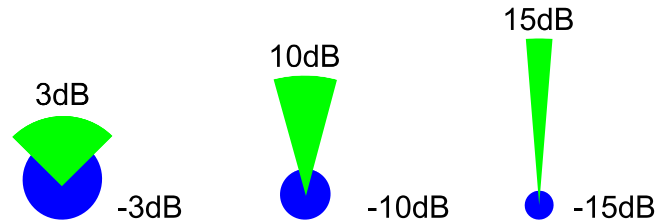

Fig. 1: An illustration of the sectored antenna model we use. While each antenna is quite directional (90°, 30°, and 9°, respectively), the amount of interference present in the network is not negligible. The network can still be interference limited.

the origin will either be LOS or NLOS. The distinction between NLOS and LOS is supported by empirical measurements conducted in Austin and Manhattan that show a differing path-loss exponent for each type of transmitter [8, 13]. The path-loss exponent on each interfering link is a discrete random variable described by

$$\alpha_{\text{i}} = \begin{cases} \alpha_{\text{L}} & \text{w.p. } \; p(r) \\ \alpha_{\text{N}} & \text{w.p. } \; 1 - p(r) \end{cases}, \tag{4}$$

where α_L, α_N are the LOS and NLOS path-loss exponents, respectively, and r is the distance from the transmitter to the receiver of interest. It was shown that by using a random shape model of buildings to model blockage [14], the probability that a communication link is LOS is $\mathbb{P}[\text{LOS}] = e^{-\beta r}$,where β is a parameter related to the dimension and density of buildings, and d is the link length. For simplicity, we ignore correlation of LOS probabilities among links, as in [14]. It was shown that the difference in the performance analysis is small when ignoring the correlation [14]. Another example is the LOS-ball approach used in [3] which treats all interfering transmitters inside a certain radius as LOS and all outside as NLOS.

Gamma fading is assumed for each interfering transmitter. In the measurements of [8, 13], small-scale fading is not a strong phenomenon. We model the fading power as a Gamma random variable with parameter N_h [3].

When discussing network density, λ is given as users/m^2 (e.g. 5×10^{-5}). We believe it is useful to relate the network density in terms of a more intuitive quantity: how far apart the users are from one another. The average *neighbor* distance of a PPP in $\mathbb{R}^2$ is given as $d_{\text{n}} := \frac{1}{2\sqrt{\lambda}}$ [9].

3. INR ANALYSIS

We are interested in analyzing the INR. Specifically,

$$P^{\text{NL}}(T) = \mathbb{P}[\text{INR} < T]. \tag{5}$$

We leave the threshold value up to system designers to determine what value of T is appropriate for defining noise limited. A natural choice may be 1 (0dB) or 10 (10dB). Using

(2),

$$P^{\mathrm{NL}}(T) = \mathbb{P}\left[\frac{\sum_{\mathrm{i}\in\Phi} P_{\mathrm{t}} M_{\mathrm{i}} h_{\mathrm{i}} A r_{\mathrm{i}}^{-\alpha_{\mathrm{i}}}}{N_0} < T\right] \quad (6)$$

$$= \mathbb{P}\left[C > \frac{\sum_{\mathrm{i}\in\Phi} P_{\mathrm{t}} M_{\mathrm{i}} h_{\mathrm{i}} A r_{\mathrm{i}}^{-\alpha_{\mathrm{i}}}}{T N_0}\right] \quad (7)$$

$$= \mathbb{P}\left[C > \frac{I_\Phi}{T N_0}\right] \quad (8)$$

$$= 1 - \mathbb{P}\left[C < \frac{I_\Phi}{T N_0}\right] \quad (9)$$

where $C = 1$ is a constant and the total interference field power given by I_Φ. We approximate the constant C as a Gamma random variable to facilitate analysis with large parameter N as $\lim_{N\to\infty} \frac{N^N x^{N-1} e^{-Nx}}{\Gamma(N)} = \delta(x)$, which is the PDF of a Gamma random variable. Further, we leverage the tight upper bound of a Gamma random variable $\mathbb{P}[g < \gamma] < (1 - e^{-a\gamma})^N$ with $a = N(N!)^{-1/N}$ [15]. The INR distribution can then be approximated as

$$P^{\mathrm{NL}} \approx 1 - \mathbb{E}_\Phi\left[\left(1 - e^{-a\frac{I_\Phi}{TN_0}}\right)^N\right] \quad (10)$$

$$= \sum_{n=1}^{N} \binom{N}{n} (-1)^{n+1} \mathbb{E}_\Phi\left[e^{-an\frac{I_\Phi}{TN_0}}\right], \quad (11)$$

where (11) is from the Binomial Theorem. The total interference field I_Φ is $I_{\Phi_{\mathrm{LOS}}} + I_{\Phi_{\mathrm{NLOS}}}$ by the Thinning Theorem [9], and are thus independent. Because the correlation between each random blockage is ignored, the building blockage is an independent which permits the use of the Thinning Theorem from stochastic geometry. Further, because we model the antenna gain between the typical receiver and each interfering user as an independent random variable, we can leverage the notion of *mark* from stochastic geometry to further split the Poisson point process. Essentially, we can now view the interference as 6 independent PPPs such that

$$I_\Phi = I_{\Phi_{\mathrm{LOS}}}^{MM} + I_{\Phi_{\mathrm{LOS}}}^{Mm} + I_{\Phi_{\mathrm{LOS}}}^{mm} + I_{\Phi_{\mathrm{NLOS}}}^{MM} + I_{\Phi_{\mathrm{NLOS}}}^{Mm} + I_{\Phi_{\mathrm{NLOS}}}^{mm}, \quad (12)$$

with the superscripts representing the discrete random antenna gain defined in (3) and each interfering node either a LOS transmitter or NLOS transmitter. Because each subprocess is independent, we can re-write (11) as a product of expectations. The form of each expectation in is the Laplace transform of the Poisson point process. We can analytically represent the first Laplace expectation term as

$$\mathbb{E}\left[e^{-\frac{an}{N_0 T} I_{\Phi_{\mathrm{LOS}}}^{MM}}\right] = e^{-2\pi\lambda p_{\mathrm{MM}} \int_0^\infty (1 - \mathbb{E}_h\left[e^{-\frac{anP_t AMMh}{r^\alpha N_0 T}}\right]) p(r) r \mathrm{d}r}, \quad (13)$$

where $(\frac{\theta}{\pi})^2$ is the probability of having antenna gain MM and $p(r)$ is the probability of being LOS. Notice that $\mathbb{E}_h[e^{\eta h}]$ corresponds to the moment-generating function (MGF) of the random variable h, which is modeled as a Gamma with parameter N_h which has a known MGF. The final Laplace transform of the PPP is given as

$$\mathcal{L}_{I_{\Phi_{\mathrm{LOS}}}^{MM}} = e^{-2\pi\lambda p_{\mathrm{MM}} \int_0^\infty \left(1 - 1/(1 + \frac{anP_t AMM}{r^\alpha N_0 T N_h})^{N_h}\right) p(r) r \mathrm{d}r}. \quad (14)$$

Each other Laplace transform is computed similarly but p_{MM} will the correspond to the probability of the antenna gain $\{MM, Mm, mm\}$ and the NLOS probability is $1 - p(r)$. We can summarize our results in the following theorem.

Theorem 1. *The instantaneous INR distribution of a mmWave ad hoc network can be tightly approximated by*

$$P^{\mathrm{NL}}(T) \approx \sum_{n=1}^{N} \binom{N}{n} (-1)^{n+1} e^{-2\pi\lambda(W+Z)} \quad (15)$$

where

$$W = \sum_i p_i \int_0^\infty \left(1 - 1/\left(1 + \frac{anP_t AM_i}{r^\alpha N_0 T N_h}\right)^{N_h}\right) p(r) r dr \quad (16)$$

and

$$Z = \sum_i p_i \int_0^\infty \left(1 - 1/\left(1 + \frac{anP_t AM_i}{r^\alpha N_0 T N_h}\right)^{N_h}\right) \left(1 - p(r)\right) r dr \quad (17)$$

with $i \in \{MM, Mm, mm\}$.

Proof. Substituting the Laplace transform (14) into (11) yields the result. □

The result allows system designers to determine the statistics of the interference as a function of antenna pattern, transmitter density, and building blockage. By understanding the statistics of the interference, designers can determine if more complicated interference reduction schemes are needed.

4. NUMERICAL RESULTS

In this section we compare Theorem 1 to a Monte Carlo simulation. These results can be used to gain intuition on when the noise power is greater than the interference power (e.g. T = 1 (0dB)). We use three antenna beamwidths in our analysis. A beamwidth of 90° would correspond to a mmWave device in a beam alignment mode or neighbor discovery. Both 30° and 9° beamwidths would correspond to data transmission mode; 9° might be used in a more stationary environment whereas 30° would be in a more mobile scenario. In all the results, we fix N_0 to -70dBm. We consider a path-loss intercept of -60dB which was shown for 28GHz [8]. The standard thermal noise for a 2GHz device (e.g. the BW of 802.11ad) at room temperature is -81dBm which leaves 11dB for an additional loss throughout the device. We assume the transmit power is 30dBm. We believe this is a pessimistic value. We show 3 different transmitter densities which correspond to a neighbor distance of approximately 15m, 22m, and 50m. We use the random boolean blockage scheme from [3] where the probability of blockage is $e^{-\beta r}$ with the building density parameter β, set to 0.008 which is based on the UT Austin campus.

Figs. 2, 3, and 4 show the instantaneous INR CDF for three values of λ for each of the beam patterns in

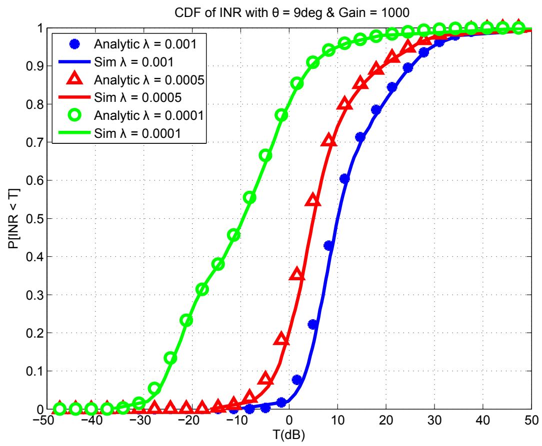

Fig. 2: The INR CDF for $\theta = 9°$. With extreme beamforming, the network remains interference limited in all but the sparest network.

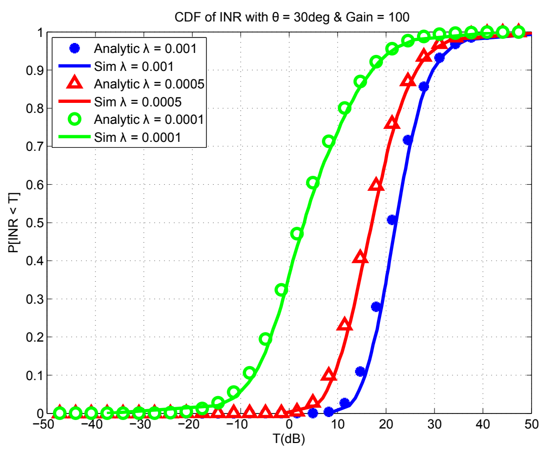

Fig. 3: The INR CDF for $\theta = 30°$. In the sparest network, the interference power is more dominant than the noise power (i.e. $\mathbb{P}[\text{INR} < 0\text{dB}] = 0.4$ for the green circle network), but the red triangle curve shows that the network is always interference limited.

Fig. 1. Indeed, in all antenna patterns, the sparsest network exhibits noise limited behavior. For example, the $\mathbb{P}[\text{INR} < 0\text{dB}] = 0.5$ for $30°$ antennas in the sparsest network. On the other hand, these results show compelling evidence that a mmWave ad hoc network can still be considered interference limited. In dense networks (22m and 70m spacing), in all but the very narrow beam case, the network exhibits strong interference. Because of this, we urge caution when considering mmWave networks to be noise limited.

Fig 5 shows the instantaneous INR distribution if we ignore NLOS interference for when $\theta = 30°$. It shows that for many mmWave networks the interference is largely driven by the LOS interference in the two denser networks. The CDF of the two denser networks in Fig. 5 is nearly identical to Fig. 3 which indicates that NLOS interference plays no role at those densities. We believe this shows compelling

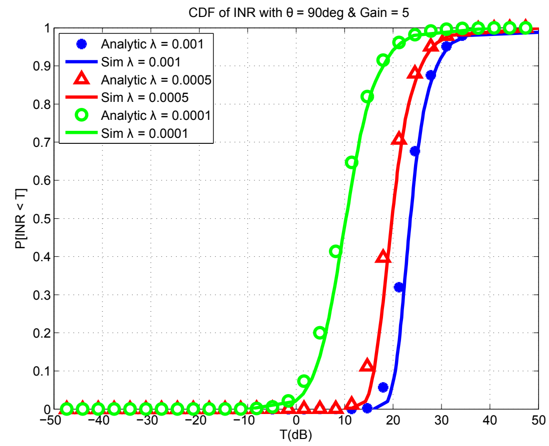

Fig. 4: The INR CDF for $\theta = 90°$. In all networks, the interference power is nearly always more dominant than the noise power (i.e. $\mathbb{P}[\text{INR} < 0\text{dB}] = 0.05$ for the green circle network).

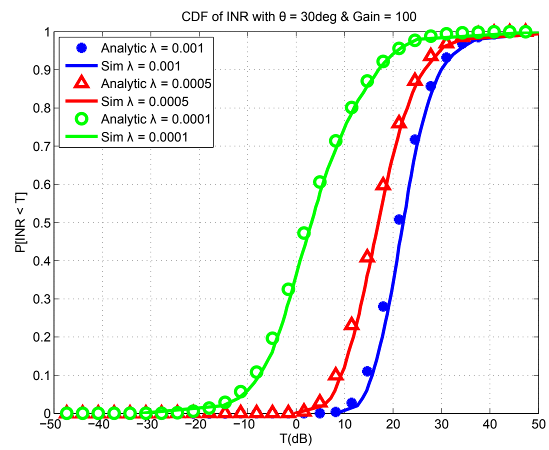

Fig. 5: The INR CDF for $\lambda = 5 \times 10^{-5}$ and $\theta = 30°$ with only LOS interference. Compared to Fig. 3, we find that the shape of INR distributions is largely determined by the LOS interference when the network is dense.

evidence that interference reduction schemes will be useful, even at mmWave frequencies. In particular, eliminating LOS interference is most important.

5. CONCLUSION

We presented an analytical characterization of the instantaneous INR distribution of a mmWave ad hoc network. We showed that mmWave networks are indeed still interference limited and are primarily *LOS interference limited*. Interference power is often, with densities of transmitter spacing under 100m, stronger than the noise power. This motivates novel mmWave architectures to deal with LOS interference in order to realize networks with achievable gigabit speeds.

6. REFERENCES

[1] "IEEE Standard for Information technology–Telecommunications and information exchange between systems–Local and metropolitan area networks–Specific requirements-Part 11: Wireless LAN Medium Access Control (MAC) and Physical Layer (PHY) Specifications Am," 2012.

[2] T.S. Rappaport, R. W. Heath Jr., R. C. Daniels, and J. Murdock, *Millimeter Wave Wireless Communications*, Prentice-Hall, September 2014.

[3] T. Bai and R.W. Heath, "Coverage and rate analysis for millimeter-wave cellular networks," *IEEE Trans. Wireless Commun.*, vol. 14, no. 2, pp. 1100–1114, Feb. 2015.

[4] J. G. Andrews, S. Buzzi, W. Choi, S. V. Hanly, A. Lozano, A. C. K. Soong, and J. C. Zhang, "What Will 5G Be?," *IEEE Journal on Selected Areas in Communications*, vol. 32, no. 6, pp. 1065–1082, June 2014.

[5] X. Zhu, A. Doufexi, and T. Kocak, "Throughput and coverage performance for IEEE 802.11ad millimeter-wave WPANs," in *Proc. of 2011 IEEE 73rd Vehicular Technology Conference (VTC Spring)*, 2011, pp. 1–5.

[6] S. Singh, R. Mudumbai, and U. Madhow, "Interference Analysis for Highly Directional 60-GHz Mesh Networks: The Case for Rethinking Medium Access Control," *IEEE/ACM Trans. Netw.*, vol. 19, no. 5, pp. 1513–1527, 2011.

[7] Y. Niu, Y. Li, D. Jin, L. Su, and D.O. Wu, "Blockage Robust and Efficient Scheduling for Directional mmWave WPANs," *IEEE Transactions on Vehicular Technology*, vol. PP, no. 99, pp. 1–1, 2014.

[8] T.S. Rappaport, Shu Sun, R. Mayzus, Hang Zhao, Y. Azar, K. Wang, G.N. Wong, J.K. Schulz, M. Samimi, and F. Gutierrez, "Millimeter Wave Mobile Communications for 5G Cellular: It Will Work!," *IEEE Access*, vol. 1, pp. 335–349, 2013.

[9] F Baccelli and B. Blaszczyszyn, *Stochastic Geometry and Wireless Networks, Volume I - Theory*, vol. 1, NoW Publishers, 2009.

[10] A. Thornburg, T. Bai, and R. W. Heath Jr., "Coverage and Capacity of mmWave Ad Hoc Networks," *To appear 2015 IEEE International Conference on Communications (ICC)*, 2015.

[11] T. Bai, A Alkhateeb, and R. W. Heath Jr., "Coverage and capacity of millimeter-wave cellular networks," *IEEE Communications Magazine*, vol. 52, no. 9, pp. 70–77, September 2014.

[12] A.M. Hunter, J.G. Andrews, and S. Weber, "Transmission capacity of ad hoc networks with spatial diversity," *IEEE Trans. Wireless Commun.*, vol. 7, no. 12, pp. 5058–5071, 2008.

[13] T.S. Rappaport, E. Ben-Dor, J.N. Murdock, and Yijun Qiao, "38 GHz and 60 GHz angle-dependent propagation for cellular amp; peer-to-peer wireless communications," in *Proc. of 2012 IEEE International Conference on Communications (ICC)*, 2012, pp. 4568–4573.

[14] T. Bai, R. Vaze, and R. W. Heath Jr., "Analysis of Blockage Effects on Urban Cellular Networks," *IEEE Transactions on Wireless Communications*, vol. 13, no. 9, pp. 5070–5083, Sept 2014.

[15] H. Alzer, "On Some Inequalities for the Incomplete Gamma Function," *Mathematics of Computation*, vol. 66, 1977.